# Processing single crystal diamond with $N_2$-GCIB: on the understanding of irradiation angle dependence on the machined surfaces

**Ke Ge Xie[1], Yuan Xie[1] and Hui Deng[1,#]**

1 Department of Mechanical and Energy Engineering, Southern University of Science and Technology, 1088 Xueyuan Avenue Shenzhen 518055, P.R.China
# Corresponding Author / Email: Dengh@sustech.edu.cn, TEL: +86-136-4140-0623

KEYWORDS: Single crystal diamond, Gas cluster ion beam, *Irradiation angles* , Materials removal rate, Roughness

*Single Crystal Diamond (SCD), renowned for its exceptional mechanical, thermal, and optical properties, occupies a pivotal position in diverse applications. Its unparalleled hardness and superior thermal conductivity render it indispensable for precision cutting tools and semiconductor devices. Recent strides in single crystal diamond synthesis and polishing methodologies have catalyzed breakthroughs in quantum computing and biomedical devices, elevating performance across scientific and industrial realms. In our investigation, we scrutinized the influence of Gas Cluster Ion Beam (GCIB) irradiation angles on the machined surface of diamond under 20 keV acceleration energy with a dose of $5\times10^{16}$ ions/cm$^2$. Employing a White Light Interferometer (WLI), we assessed material removal rates by selectively masking half of the diamond surface. Remarkably, $N_2$-GCIB exhibited maximal material removal efficiency at normal incidence angles, with diminishing rates as the angle deviated from the perpendicular. Intriguingly, minimal material ablation occurred when the incidence angle surpassed 80 degrees. Furthermore, we delved into the angle-dependent surface roughness (Ra and Rq) on both machined and non-machined surfaces. Leveraging White Light Interferometer (WLI) measurements and Atomic Force Microscopy (AFM), we observed reductions in both Ra and Rq following irradiation at varying angles. Notably, Rq exhibited less sensitivity to incidence angle variations, while Ra displayed a significant decline. These findings enhance our comprehension of single crystal diamond behavior under controlled irradiation conditions, yielding valuable insights for practical applications. The interplay between irradiation angles and material removal rates provides a foundation for optimizing diamond machining processes, paving the way for continued advancements in cutting-edge technologies.*

## 1. Introduction

Single Crystal Diamond (SCD), renowned for its exceptional mechanical, thermal, and optical properties, occupies a pivotal position in diverse applications. Its unparalleled hardness and superior thermal conductivity render it indispensable for precision cutting tools and semiconductor devices. Recent strides in single crystal diamond synthesis and polishing methodologies have catalyzed breakthroughs in quantum computing and biomedical devices, elevating performance across scientific and industrial realms [1]. Despite the promising application prospects, the precise processing of SCD in an efficient manner keeps presenting challenges. So far, plenty of methods have been proposed to improve the processing [2], e.g., mechanical, chemical-mechanical, dynamic friction polishing and plasm-assisted polishing. However, no single method can meet all the requirements of modern ultra-precision polishing. GCIB technology is proposed among the various processing technologies by scientists in their exploration of new polishing techniques [3], which is considered to be an innovative solution with the absolute advantages of being green, efficient and cost-saving.

During the past decades, considerable work has been carried out on GCIB processing, from gas types [4], acceleration energy [5], via irradiation dose [3], to incidence angles [6]. Among them, acceleration energy and irradiation dose have been intensively studied, and fairly linear relationships have been revealed. By contrast, the dependence on gas types and irradiation angle are kept being explored. Meanwhile, few works are being carried out on SCD processing with GCIB.

Specifically, there are some leading progresses regarding diamond processing with GCIB. Toyoda et al. [7] studied the irradiation effect of Ar and $O_2$ cluster ion beams on CVD diamond films. They found that the diamond surface roughness decreased with the Ar cluster while a thin graphite layer was formed as well. When it came to the $O_2$ cluster, neither the roughness was improved, nor the graphite layer was formed. Greer et al. [5] AFM images for a polycrystalline diamond film before and after processing with a high dose of $1.4\times10^{17}$ ions/cm$^2$ at 20 keV. This dose significantly reduced the surface roughness of this film, from

29 nm down to 9.4 nm. More recently, Wang et al. [8] used Ar and $SF_6$-Gas cluster ion beams to polish CVD diamond for direct bonding, finding that Ar-GCIB could change the diamond morphology and at the same time decrease the surface roughness, while $SF_6$-Gas caused the roughness to decrease slightly. With surface roughness reducing from 334 nm to 0.5 nm, the polished substrate was successfully bonded to GaN using surface-activated bonding with a Si nano-layer.

With the understanding to the existing work performed, it shows that both $N_2$-GCIB and irradiation angles dependences are studied on SCD. In this work, we analysed the mechanisms of GCIB process and irradiation angles dependence. By performing experiments, we studied the SCD removal rate and surface roughness changed with irradiation angles of $N_2$-GCIB.

## 2. Theoretical analysis

### 2.1 Mechanism of GCIB process

As shown in Fig.1, compressed source gases flow through a tube after gas regulation. When the gases come through a special nozzle into a vacuumed environment, adiabatic expansion and collision happen, and gas clusters are generated. The clusters will be firstly filtered by a skimmer, and then be ionized, accelerated by ionizer and electron accelerator respectively. Following an analysis magic, electrons and small clusters will be blocked, while clusters with proper size will pass through an aperture after neutralization. The eventual gas cluster ion beam irradiated the whole workpiece surface with stage movements.

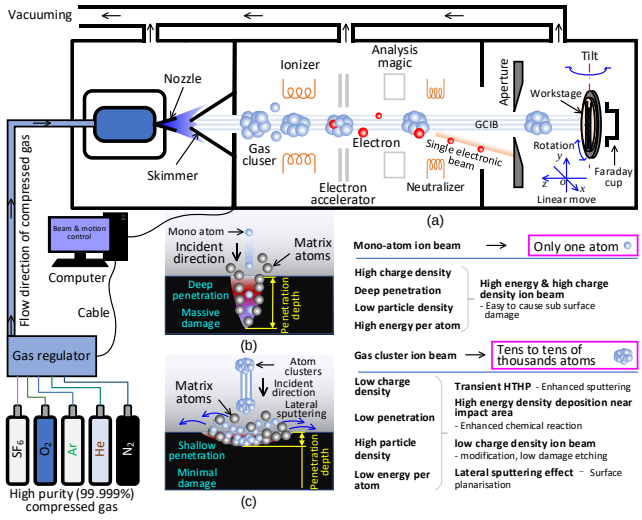


Fig. 1 GCIB technology. (a) Mechanism of GCIB. Differences betwe en mono-atom ion beam (b) and (c) GCIB.

Different to mono-atom ion beam, which has only one atom, GCIB contains tens to tens of thousands of atoms. Compared to mono-atom ion beams, GCIB has a low charge density, low penetration depth, low energy per atom, but high particle density. These features make GCIB ideally suited for plenty of applications, e.g., (i) enhanced sputtering and chemical reactions thanks to the transient HTHP and the high energy density deposition near the impact area, and (ii) surface modification, low-damage etching and surface planarization owing to the low charge density ion beam and the unique lateral sputtering effect.

### 2.2 Irradiation angle dependence

The dependence of irradiation angles has been studied for many materials, including metal materials [3, 9], oxide [10], and semiconductors [11]. Interestingly, it has been revealed and validated in some of the research that nanopatterns can be formed at oblique incidence angles of 30°-70°, and these nano-waves are perpendicular to the incident direction [11].

Fig.2 shows the schematic diagram of incline irradiations. Yamada et al. [3] studied the angular distribution of sputtered Cu atoms under different conditions. It indicates that even at an oblique incidence angle of only 10°, most of the sputtered particles were distributed in the forward direction. No notable change in the angular distribution was found when the angle of incidence was changed from 10° to 60°. Aoki and Matsuo [12] used molecular dynamics simulations to study the GCIB collisional process. It revealed that certain angles cause crater-like damage, while larger angles allow the cluster to slide without displacement. These findings indicated that large irradiation angles could be potentially used to smooth the substrate surface without damaging it.

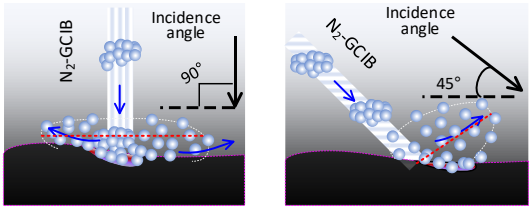


Fig. 2 Schematic diagram of incline irradiation. (a) normal irradiation, (b) incline irradiation.

## 3. Experimental study

### 3.1 Experimental strategies

Fig.3 shows the experimental strategies employed in this work. A total of five SCD samples were used in the experiments, which were received from Hebei Plasma Diamond Technology Co., Ltd. All the top surfaces (crystal face (100)) of the samples were pretreated by the CMP method, and each block size was 10×10×1 mm. As shown in Fig.3(a), the sample was attached to the work stage via conductive tape, and the top half of the sample was covered during the GCIB processing. The main motion during the processing is the Y-axis. The five samples were sequentially processed by different GCIB irradiation angles ranging from 0° to 80° with an interval of 20°, respectively. The moving route was designed to cover the whole sample, and each time the GCIB focal spot fully moved out of the sample surface (see Fig.3b). Fig.3(c) shows the GCIB equipment used in the experiment, which is manufactured by IIPT Inc. from Japan. After $N_2$-GCIB with different irradiation angles bombarded (acceleration energy: 20 keV, dose: $5\times10^{16}$ ions/cm$^2$), the masks on the samples were carefully removed by hand, and then the samples were cleaned by an ultrasonic cleaner in the acetone and alcohol environments for 10 minutes, respectively. Finally, the samples were dried by dry air. Fig.3(d) shows the details of the experimental results and measurement equipment used in this work. The whole topography of the sample surface was obtained at an

irradiation angle of 0° via the built-in functions of WLI (CCI, Taylor Hobson, see Fig.3d2). Then, both the masked and processed areas were measured at three selected positions (see Fig.3d1). Wherein, the gray square frame indicated the areas measured by WLI, and the black dot represented the areas measured by AFM (Dimension Edge, Bruker, see Fig.3d3). The displayed roughness values were the averages of the three selected positions.

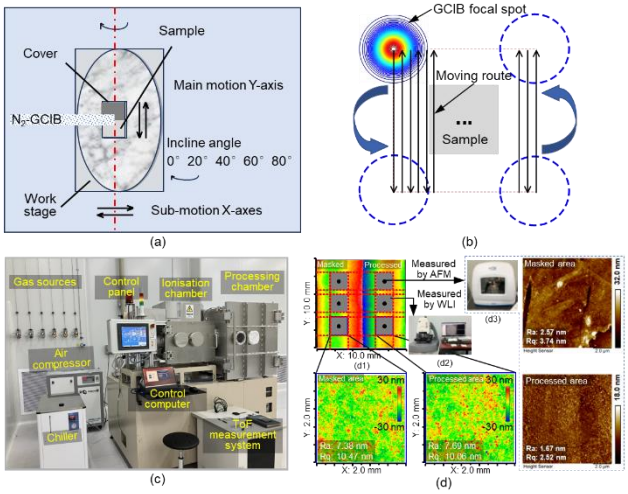


Fig. 3 Experimental strategy. (a) placement and treatment of samples. (b) Irradiation area and route. (c) GCIB equipment. (d) Evaluation methods.

## 3.2 Experimental results and analysis

### 3.2.1 Incidence angle dependence on material removal rate

By further using the built-in functions of WLI, the differences between the masked and processed surfaces at Y = 2.5 mm, 5.0 mm, and 7.5 mm were achieved, as shown in Fig. 4.

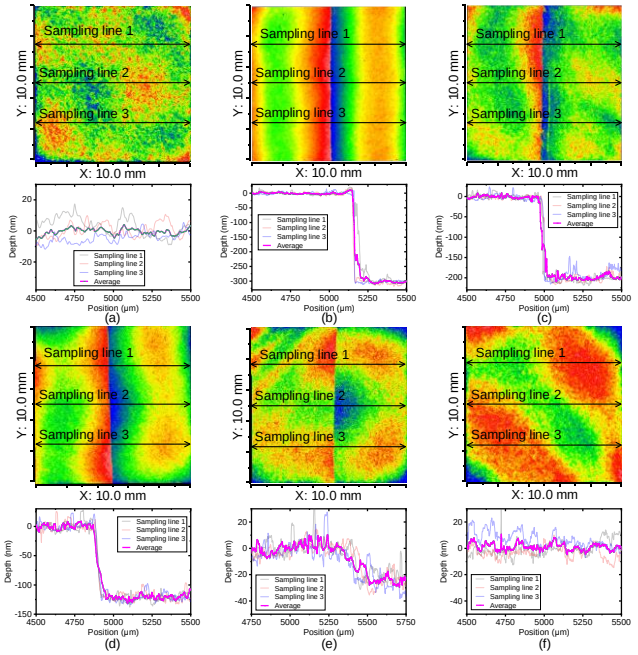


Fig. 4 Incidence angle dependence on material removal rate. (a) original surface. Surfaces processed by (b) 0°, (c) 20°, (d) 40°, (e) 60° and (f) 80° irradiation angle.

It showed that the sample was almost flat before irradiation (see Fig.4a). However, after $N_2$-GCIB bombarded, a clear boundary appeared between the masked and the processed areas when the irradiation angles ranged from 0° to 60° (see Fig.4b-e). Besides, the differences between the masked and processed areas decreased with the incidence angle, and no identifiable boundary line could be found when the incidence angle exceeded 80° (see Fig.4f).

Fig. 5 shows the comparisons of different incidence angles effects on the material removal rate. It showed that the material removal rate was the highest when the irradiation angle was zero, about 300 nm per 5E16 ions/cm$^2$. With the increasing incline angle, the material removal rate approximately linearly decreased until 60°, where the removal rate started suddenly slowing down. When the incline angle was 80°, no material removal could be found. These phenomena might be due to the dominant difference in energy deposition. When the irradiation angle was small, a large part of the deposited energy on the target atom was used to create the surface crater. However, when the incident angle exceeded 60°, the most kinetic energy was used to break up the cluster itself, which has been proven by Aoki and Matsuo' simulation work [12].

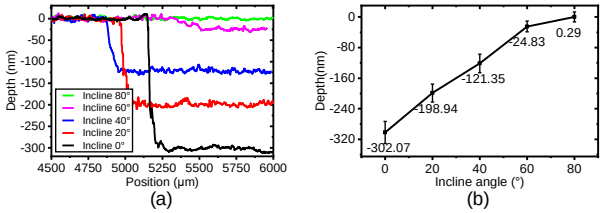


Fig. 5 Comparison of different incidence angles effect on the material removal rate. (a) comparisons of the results. (b) tendency of material removal rates changes with irradiation angles.

### 3.2.2 Incidence angle dependence on surface roughness

Both the surface roughness measured by WLI and AFM were used to study the incidence angle dependence in this work. It was shown from the WLI results that the roughness changed little after processing under different irradiation angles (as shown in Fig. 6). The biggest change was in Fig.6(d), where the Ra showed a roughly 30% drop. As for Rq, the drop was minimal despite the decreasing tendency under all the irradiation angles.

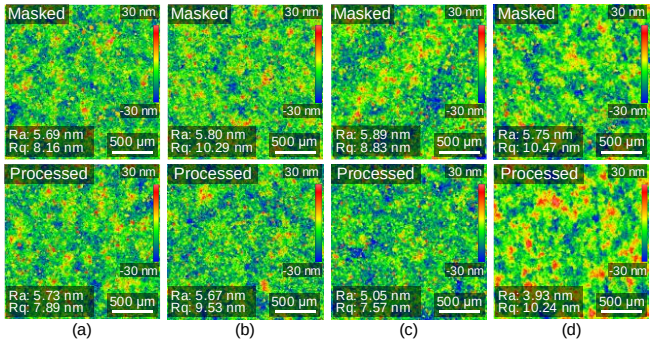


Fig. 6 Incidence angle dependence on surface roughness measured by WLI. Results of masked and processed area under the irradiation angle of (a) 20°, (b) 40°, (c) 60° and (d) 80°.

The results measured by AFM showed that both Ra and Rq were dropped after irradiation under different incline angles (as shown in Fig. 7). Notably, thanks to the lateral sputtering effect, defects like cracks and scratches were not found under small incline angles. Meanwhile, these defects tend to appear as the incidence angle increases. These findings indicated that small irradiation angles would be more suitable for repairing the defective SCD surface.

Most interestingly, it was reported for most of the materials that nanoscale patterns would be formed by GCIB when the irradiation angles ranged from 30° to 70° [11]. However, no identifiable regular patterns were found, with the incidence angle changing from 30° to 80° during our study. Therefore, it could be inferred from the conclusion that irradiation angle was not the only factor that influenced the formation of nanoscale patterns.

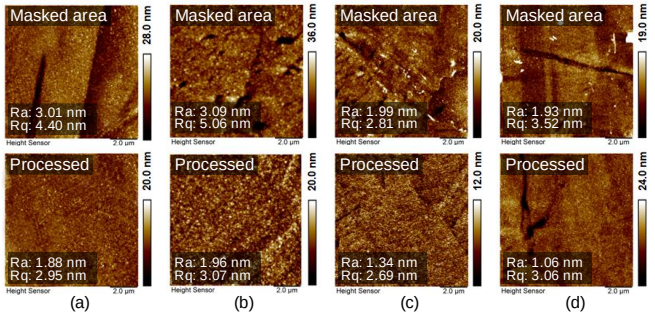


Fig. 7 Incidence angle dependence on surface roughness measured by WLI. Results of masked and processed area under the irradiation angle of (a) 20°, (b) 40°, (c) 60° and (d) 80°

Fig.8 shows the comparisons of different incidence angles effects on the surface roughness, in which, both the WLI (intermediate frequency roughness) and AFM (high frequency roughness) results revealed that the Ra decreased with incidence angle, but the correlation between Rq and incident angle was weak. Meanwhile, results from AFM showed a clear drop in both Ra and Rq. It indicated that the $N_2$-GCIB played a more important role in surface smoothing than flattening.

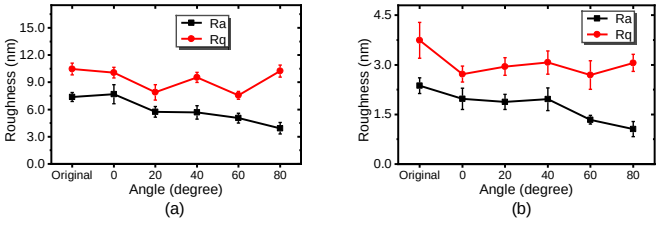


Fig. 8 Comparisons of different incidence angles affect the surface roughness. (a) Results from WLI. (b) Results from AFM.

## 4. Conclusions

GCIB was a newly developed technology that could be used to process many materials for various purposes. Yet, there were lots of laws that kept being revealed. This paper investigated the processing of SCD with $N_2$-GCIB under different irradiation angles. The key conclusions from this paper were drawn as follows:

1) $N_2$-GCIB has a higher material removal rate when the irradiation angle is small. The material removal rate close to linearly decreases with the incidence angle increasing to 60°, then the removal rate gradually decreases to zero.

2) Irradiation angle change is not the only factor that affects the formation of nanoscale patterns. Nevertheless, there is a clear correlation between the incidence angle and the surface defects.

3) SCD surface Ra is a correlate of irradiation angle, while the relationship between Rq and irradiation angle is not strongly correlated.

## ACKNOWLEDGEMENT

The authors acknowledge the support of the National Natural Science Foundation of China (NSFC) [grant number 52035009].

## REFERENCES

1. Liu, W., et al., "Highly efficient and atomic-scale smoothing of single crystal diamond through plasma-based atom-selective etching," Diamond and Related Materials, Vol. 143, No. pp. 110840, 2024.
2. Luo, H., et al., "Polishing and planarization of single crystal diamonds:state-of-the-art and perspectives," International Journal of Extreme Manufacturing, Vol. 3, No. 2, pp. 44-87, 2021.
3. Yamada, I., et al., "Materials processing by gas cluster ion beams," Materials Science and Engineering: R: Reports, Vol. 34, No. 6, pp. 231-295, 2001.
4. Guo, E.-F., et al., "Study of argon/hydrogen mixed cluster in supersonic gas jet," Acta Physica Sinica, Vol. 63, No. 10, pp. 103601, 2014.
5. Greer, J.A., et al., "Etching, smoothing, and depositon with gas_cluster ion beam technology," Surf Coat Tech, Vol. 133-134, No. 2000, pp. 273-282, 2000.
6. Toyoda, N. and I. Yamada, "Gas Cluster Ion Beam Equipment and Applications for Surface Processing," IEEE Transactions on Plasma Science, Vol. 36, No. 4, pp. 1471-1488, 2008.
7. Toyoda, N., et al., "Surface treatment of diamond films with Ar and O2 cluster ion beams," Nuclear Instruments and Methods in Physics Research Section B: Beam Interactions with Materials and Atoms, Vol. 148, No. 1, pp. 639-644, 1999.
8. Wang, J., et al. "Polishing Diamond Substrates using Gas Cluster Ion Beam (GCIB) Irradiation for the Direct Bonding to Power Devices," 2022 International Conference on Electronics Packaging (ICEP). 2022.
9. Saleem, I., et al., "Cluster ion beam assisted fabrication of metallic nanostructures for plasmonic applications," Nucl Instrum Methods Phys Res Sect B, Vol. 380, No. pp. 20-25, 2016.
10. Zeng, X.-M., et al., "Design and application of gas cluster accelerator for surface smoothing and nanostructures formation," Acta Physica Sinica, Vol. 69, No. 9, pp. 2020.
11. Lozano, O., et al., "Evolution of nanoripples on silicon by gas cluster-ion irradiation," AIP Advances, Vol. 3, No. 6, pp. 2013.
12. Aoki, T. and J. Matsuo, "Molecular dynamics study of surface modification with a glancing angle gas cluster ion beam," Nucl Instrum Methods Phys Res Sect B, Vol. 255, No. 1 SPEC. ISS., pp. 265-268, 2007.